TTCGCAGCAGCCAGCACTAAACTT-3'). Each 2.2-kb Hind III fragment generated from PCR mutagenesis was then cloned into the Hind III site of pSK1.0 to obtain the mutant plasmid in *E. coli* strain DH5α. The restoration of the entire *bla* region in the correct orientation was confirmed by restriction mapping. This mutant plasmid was ligated into Sma I–digested *S. aureus* plasmid pRN5542 for transformation into *S. aureus* strain RN4220. NH_2-terminal amino acid sequence was determined by Edman degradation reaction by the University of California at San Francisco Biomolecular Resource Center.

17. G. I. Evans, G. K. Lewis, G. Ramsey, V. M. Bishop, *Mol. Cell. Biol.* **5**, 3610 (1985).
18. GST-BlaI fusion protein expression and purification were performed with the GST Gene Fusion System (Pharmacia Biotech). BlaI-GST and BlaR1-His^6 were constructed with overlapping-extension PCR (*15*) in the context of an otherwise wild-type *bla* region. A culture of recombinant *S. aureus* strain RN4220 was grown in the presence of CBAP (10 μg/ml) to induce expression of the fusion product. Cells were harvested and mechanically disrupted by glass beads in a cell homogenizer. Cleared lysates containing BlaI-GST were subject to the purification procedure by using a GST protein purification kit (Clontech). BlaR1-His^6 fusion protein was purified with the Talon Metal column purification kit (Clontech).
19. Single-letter abbreviations for the amino acid residues are as follows: A, Ala; C, Cys; D, Asp; E, Glu; F, Phe; G, Gly; H, His; I, Ile; K, Lys; L, Leu; M, Met; N, Asn; P, Pro; Q, Gln; R, Arg; S, Ser; T, Thr; V, Val; W, Trp; and Y, Tyr.
20. β-Lactamase activity was assessed with Nitrocephin discs, according to manufacturer's instructions (Becton-Dickinson).
21. N. M. Hooper, *FEBS Lett.* **354**, 1 (1994).
22. W. Jiang, J. S. Bond, *FEBS Lett.* **312**, 110 (1992).
23. C. Marie-Claire, B. P. Roques, A. Beaumont, *J. Biol. Chem.* **273**, 5697 (1998).
24. C. J. Hackbarth, C. Miick, H. F. Chambers, *Antimicrob. Agents Chemother.* **38**, 2568 (1994).
25. S. Cohen, H. M. Sweeney, *J. Bacteriol.* **95**, 1368 (1968).
26. J. S. Parkinson, *Cell* **73**, 857 (1993).
27. T. Tomoyasu *et al.*, *EMBO J.* **14**, 2551 (1995).
28. A. E. Hofmeister, A. Londono-Vallejo, E. Harry, P. Stragier, R. Losick, *Cell* **83**, 219 (1995).
29. B. Kreiswirth *et al.*, *Nature* **227**, 680 (1983).
30. R. Novick, *Methods Enzymol.* **204**, 587 (1991).
31. E. Harlow, D. Lane, *Antibodies: A Laboratory Manual* (Cold Spring Harbor Laboratory Press, Cold Spring Harbor, NY, 1988).
32. This research was supported by NIH/National Institute of Allergy and Infectious Diseases grants AI4005804 (C.J.H.) and AI46610 (H.F.C.). We are grateful for the critical review of the manuscript by P. Rosenthal and J. Ernst.

22 August 2000; accepted 15 January 2001

Recovery of Infectious Ebola Virus from Complementary DNA: RNA Editing of the GP Gene and Viral Cytotoxicity

Viktor E. Volchkov,[1,2]* Valentina A. Volchkova,[1] Elke Mühlberger,[1] Larissa V. Kolesnikova,[1] Michael Weik,[1] Olga Dolnik,[1] Hans-Dieter Klenk[1]

To study the mechanisms underlying the high pathogenicity of Ebola virus, we have established a system that allows the recovery of infectious virus from cloned cDNA and thus permits genetic manipulation. We created a mutant in which the editing site of the gene encoding envelope glycoprotein (GP) was eliminated. This mutant no longer expressed the nonstructural glycoprotein sGP. Synthesis of GP increased, but most of it accumulated in the endoplasmic reticulum as immature precursor. The mutant was significantly more cytotoxic than wild-type virus, indicating that cytotoxicity caused by GP is down-regulated by the virus through transcriptional RNA editing and expression of sGP.

Ebola virus (EBOV) is a highly dangerous pathogen causing hemorrhagic fever in humans and nonhuman primates. Mortality rates up to 90% and the lack of measures to prevent the disease classify this virus at biosafety level P4 (*1*). Together with Marburg virus (MBGV), it forms the family Filoviridae (*2*), a group of enveloped, nonsegmented, negative-stranded RNA viruses. The EBOV genome is 18,959 nucleotides (nt) in length and is transcribed into eight major subgenomic mRNAs that encode seven structural proteins and one nonstructural protein. Four of these—NP, VP35, VP30, and the catalytic subunit L of the RNA polymerase—are constituents of the ribonuleocapsid (*2*). VP40 and VP24 are matrix proteins. GP is a membrane glycoprotein that is located at the surface of EBOV-infected cells and forms the spikes on virions. Expression of GP, which is encoded by two overlapping reading frames, requires the insertion of a non–template-coded adenosine residue by a mechanism of transcriptional RNA editing (*3*, *4*). Most (about 80%) GP mRNAs are not edited, and they direct synthesis of the nonstructural glycoprotein sGP, which is secreted from EBOV-infected cells. GP and sGP are identical at their NH_2-terminal ends (295 amino acids) but differ at the COOH termini owing to the use of different reading frames. Surface GP presumably mediates virus entry by receptor binding and membrane fusion and is a determinant of cell tropism (*5*, *6*). Proteolytic cleavage of GP may play a role in pathogenesis (*7*). It has recently been reported that recombinant GP induces cell disruption and cytotoxicity and that it may therefore be a determinant of pathogenicity (*8*, *9*). Significant amounts of sGP can be detected in sera of patients suffering from EBOV hemorrhagic fever, which supports the notion that sGP also plays an important role in pathogenesis (*10*). However, MBGV, which causes disease symptoms similar to those of EBOV, expresses only GP from a single open reading frame (*11*, *12*). GP levels are low in cells infected with MBGV, although editing does not occur in this case. Therefore, the roles of transcriptional editing and of sGP in EBOV replication and pathogenesis are not well understood. The present study was undertaken to elucidate these problems.

A cDNA clone encoding the complete antigenome of the Mayinga strain of EBOV subtype Zaire (*13*), was constructed from three overlapping cDNA segments of approximately 6000 base pairs (bp) (KSN-4, KSS-25, and KSL-23), each generated from a plasmid library described elsewhere (*14*–*16*). As a marker for the rescue of recombinant EBOV (recEBOV), two nucleotide mutations at a unique Sal I restriction site were introduced into the antigenomic cDNA by means of site-directed mutagenesis (*17*). This clone, which contained the authentic editing site, was designated pFL-$EBOVe^+$. To recover recEBOVe^+, a BHK-21 cell line (BSR T7/5) stably expressing T7 polymerase under the control of a cytomegalovirus promoter (*18*), was cotransfected with pFL-$EBOVe^+$ and four plasmids encoding the nucleocapsid proteins NP, VP35, VP30, and L (*19*, *20*). A typical cytopathic effect (CPE) in the form of several foci of rounded cells was observed in cell culture dishes between 6 and 9 days after transfection. To amplify rescued virus, culture supernatants from BSR T7/5 cells were inoculated onto Vero E6 cells, where recombinant virus induced easily visible CPE 4 to 6 days after infection. When any of the plasmids expressing NP, VP35, VP30, or L was omitted, CPE was not observed in either BSR T7/5 cells or in subsequent passages on Vero E6 cells, which supports the previous observation that NP, VP35, and L are essential for

[1]Institut für Virologie, Philipps-Universität, Robert-Koch-Strasse 17, 35037 Marburg, Germany. [2]University Claude Bernard Lyon-1, Filovirus Laboratory, 21 Avenue Tony Garnier, 69365 Lyon Cedex 07, France.

*To whom correspondence should be addressed. E-mail: viktor.volchkov@ens-lyon.fr

the replication of artificial filovirus replicons and that VP30 is required for EBOV transcription (*19*, *21*). To illustrate that the CPE in BSR T7/5 cells or Vero E6 cells was indeed caused by EBOV infection, the accumulation of the matrix protein VP40 in the culture supernatants was analyzed. VP40 was detected with each plasmid clone that contained a full-length copy of the EBOV antigenome used in our rescue experiments. Similar amounts of this protein were also found in culture supernatants of cells infected with authentic EBOV (Fig. 1A). When viral RNA from culture supernatants was analyzed by reverse transcription polymerase chain reaction (RT-PCR) (*22*), the absence of the restriction site marker Sal I demonstrated the identity of recEBOVe$^+$ (Fig. 1B). In addition, the presence of the mutations at Sal I and in the 3′ noncoding region of the L gene were confirmed by sequence determination after three subsequent passages of recEBOVe$^+$ on Vero cells. recEBOVe$^+$ did not differ with respect to its growth characteristics when compared to the authentic EBOV, strain Mayinga, except for a slightly higher CPE during the early passages.

To test the potential of this reverse genetics system as a tool for the investigation of the molecular biology of EBOV, we constructed a recombinant virus in which the editing site of the GP gene was eliminated by mutation (Fig. 1C). The editing site, which consists of seven consecutive adenosine residues and is located in the middle of the gene encoding GP (AAAAAAA, antigenomic sense), resembled the EBOV polyadenylation signal (ATTAAGAAAAAA, antigenomic sequence). This suggests that editing may occur by the slippage of the viral transcriptional complex on the RNA template (*3*), as has also been described for the P genes of paramyxoviruses (*23*). We therefore changed the editing site by site-directed mutagenesis of the intermediate plasmid pKSS-25 from AAAAAAA to AAGAAGAA. Thus, two adenosines were replaced by guanosines to interrupt the polyadenosine sequence, and an additional adenosine was inserted to link the two overlapping reading frames encoding GP. The plasmid pFL-EBOVe$^-$, encoding the complete antigenome with the mutations at the editing site, was constructed essentially as described above for pFL-EBOVe$^+$ (*13*). recEBOVe$^-$ was rescued according to the protocol used for recEBOVe$^+$ (*20*). The recovered agent was again identified as recombinant virus by the absence of the Sal I marker and by the mutations at the editing site that were confirmed by sequencing of PCR fragments corresponding to the GP gene before and after plaque purification of the virus. Confirmation of the recovery of recEBOVe$^-$ was obtained after immunoblot analysis of the culture supernatants of infected cells using antibodies to sGP (Fig. 1D) or to VP40 (Fig. 1E). As expected, expression of sGP was totally blocked with recEBOVe$^-$, whereas the amount of VP40 released into the medium was comparable with either recombinant.

During the rescue process, recEBOVe$^-$ showed a significant increase in cytotoxicity when compared with recEBOVe$^+$. Cells infected with recEBOVe$^-$ began to round up and to detach 3 to 4 days after infection. After 5 to 6 days, cell rounding was complete, and most cells detached into the medium. In contrast, after infection with recEBOVe$^+$, intact monolayers were preserved for 8 days after

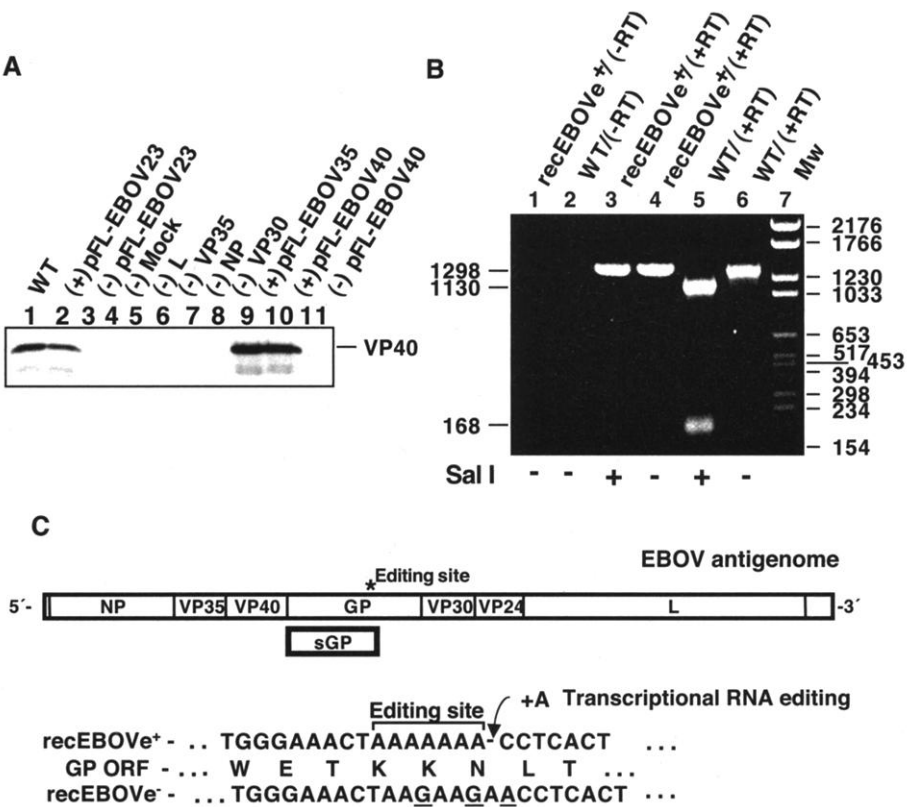

Fig. 1. Recovery of recEBOVe$^+$ and recEBOVe$^-$ from full-length antigenomic cDNAs. (**A**) The presence of EBOV VP40 in the culture supernatants from Vero E6 cells was analyzed by Western blotting using rabbit polyclonal antibodies to VP40. Vero cells were inoculated with supernatants collected from BSR T7/5 cells transfected with different mixtures of the recombinant plasmids, as indicated. Three individual plasmid clones of the full-length EBOV genome (pFL-EBOV23, pFL-EBOV35, and pFL-EBOV40) were tested for virus rescue. The presence of VP40 indicated virus recovery from cells infected with wild-type (WT) EBOV (lane 1) or transfected with any of the three templates together with plasmids expressing all four of the nucleocapsid proteins (lanes 2, 9, and 10). The absence of VP40 indicated that virus was not rescued from mock-infected cells (lane 4) when the templates were not present (lanes 3 and 11) or when any one of the plasmids expressing the four nucleocapsid proteins was not present [(−)L, (−)VP35, (−)NP, and (−)VP30, lanes 5 through 8, respectively]. (**B**) Identification of the Sal I marker mutation in the GP gene of recEBOV. Virion RNA was isolated from culture supernatants of Vero E6 cells infected with either plaque-purified recEBOVe$^-$ or authentic EBOV, strain Mayinga. RT-PCR was performed with primers that flanked the mutation region. The PCR products were subjected to restriction analysis with Sal I and separated on a 1% agarose gel. Lanes 1 and 2, PCR without the RT stage; lanes 3 and 4, RT-PCR products of recEBOVe$^+$; lanes 5 and 6, RT-PCR products of WT EBOV; lane 7, DNA marker (Mw, molecular weight). (**C**). Schematic representation of the full-length EBOV antigenomic cDNA and of nucleotide sequences at the GP gene editing site present in recEBOVe$^+$ and recEBOVe$^-$. (**D** and **E**) Recovery of recEBOVe$^-$. Vero E6 cells were infected with equal amounts of either recombinant virus or WT EBOV at a MOI of 10^{-2}, and culture supernatants were collected 4 days after infection. The presence of EBOV nonstructural sGP (D) or structural protein VP40 (E) in the culture supernatants was analyzed by Western blotting using rabbit polyclonal antibodies to sGP or VP40.

infection (Fig. 2A) or even longer, if cells were fed by addition of fresh fetal bovine serum. When growth curves were compared, replication kinetics were similar for the first 4 to 5 days, but recEBOVe$^-$ showed a significant drop in titer during the next 2 days, obviously owing to the death of infected cells (Fig. 2B). As indicated by neutral red staining, recEBOVe$^+$ plaques contained cells that were morphologically changed but still well attached and viable, whereas predominantly rounded and dead cells were found in recEBOVe$^-$ plaques. The reduced size of recEBOVe$^-$ plaques suggests that the early death of infected cells limits the spread of the virus (Fig. 2C). To confirm that the differences in growth were due to the increased cytotoxicity of recEBOVe$^-$ and the damage of cellular membranes, culture supernatants from cells infected with equal amounts of either recombinant virus were analyzed for the release of the cytosolic enzyme lactate dehydrogenase (LDH). recEBOVe$^-$ was found to induce severe cell damage, as indicated by an early and extensive increase of LDH level in the medium. With recEBOVe$^+$, a smaller LDH release was observed (Fig. 2D).

Why does cytotoxicity increase when transcriptional editing is abolished? The mutations at the editing site did not alter the amino acid sequence of GP and therefore should have no effect on its three-dimensional structure or on its function. Indeed, electron microscopy revealed that recEBOVe$^+$ and recEBOVe$^-$ particles showed the typical filovirus structure and were indistinguishable from each other (Fig. 3A) and from authentic EBOV. Immunofluorescence staining with antibodies to NP confirmed that both recEBOVe$^+$ and recEBOVe$^-$ possess similar infectivity and virus production (Fig 3B). However, there are clear differences in the expression strategies of either recombinant. With authentic EBOV carrying the wild-type editing site, only one of five transcripts of the GP gene directs synthesis of full-length GP, whereas the rest encodes sGP (*3*). A similar sGP/GP ratio was observed in cells infected with recEBOVe$^+$. In contrast, there was an excess of GP when sGP was not produced in cells infected with recEBOVe$^-$. This was clearly demonstrated by immunofluorescence (Fig. 3C), as well as by Western blot analyses (Fig. 3D, left panel). The increase in GP expression, however, did not result in a simultaneous increase in virus release, as was demonstrated by the growth curves (Fig. 2B) and by the immunoblotting analysis of the culture supernatants (Figs. 1E and 3D, right panel). Moreover, most of the GP synthesized under these conditions was immature precursor with sugar side chains of the high-mannose type, which are sensitive to treatment with endoglycosidase H (Fig. 3D, left panel). This indicates that GP transport was arrested in the endoplas-

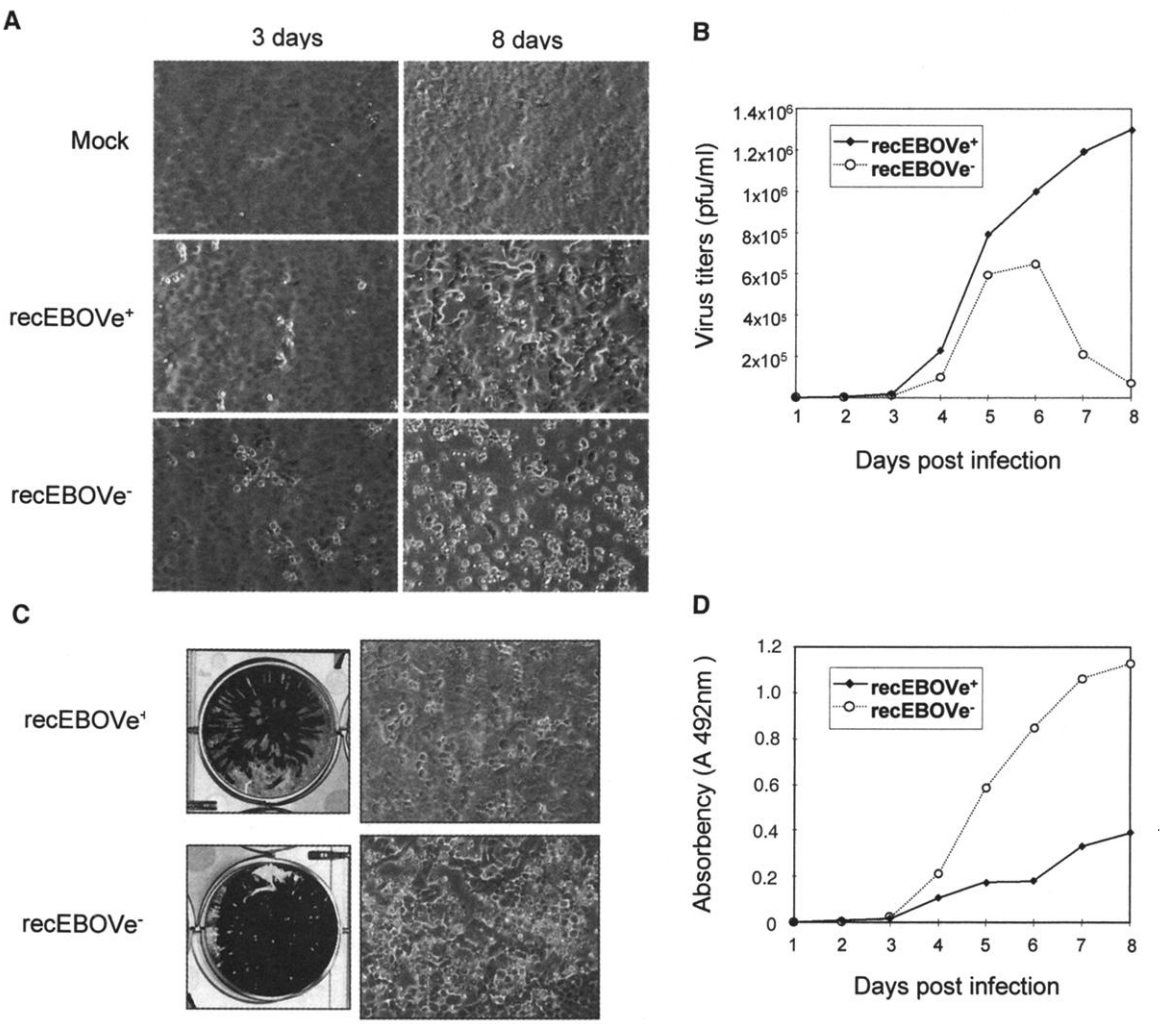

Fig. 2. Cytopathogenicity of recEBOV in Vero E6 cells. (**A**) Cells infected with the indicated viruses were observed under a light microscope for 8 days after infection. The progress of the infection was monitored until complete CPE was observed with recEBOVe$^-$. recEBOVe$^+$ induced moderate CPE with small foci or only isolated degenerating cells. No visible CPE was observed with mock-infected cells for at least 8 days. (**B**) Kinetics of multicycle growth of recEBOVe$^+$ and recEBOVe$^-$. Monolayers of Vero E6 cells were infected at a MOI of 10^{-2}, and aliquots of culture media were harvested at 24-hour intervals for 8 days. Samples were analyzed by plaque assay in duplicate using a protocol previously described (*26*). Data are means of two separate experiments, and deviation was less than 5%. pfu, plaque-forming units. (**C**) Plaques formed by recEBOVe$^+$ and recEBOVe$^-$. Vero E6 cells were inoculated with culture supernatants from BSR T7/5 cells transfected with cDNAs encoding EBOV antigenomes and NP, VP35, VP30, and L proteins. The cells were overlaid with agar and incubated for 5 days at 37°C. Individual plaques were visualized after staining with neutral red (right panels). Plates were then stained with 0.1% crystal violet in a 10% formaldehyde solution (left panels). A marked reduction in plaque size was observed with the editing site mutant recEBOVe$^-$ as compared to recEBOVe$^+$. (**D**) Kinetics of LDH release from EBOV-infected Vero E6 cells. Culture medium from multicycle growth experiments was centrifuged at low speed and analyzed by the cytotoxicity detection kit (Roche).

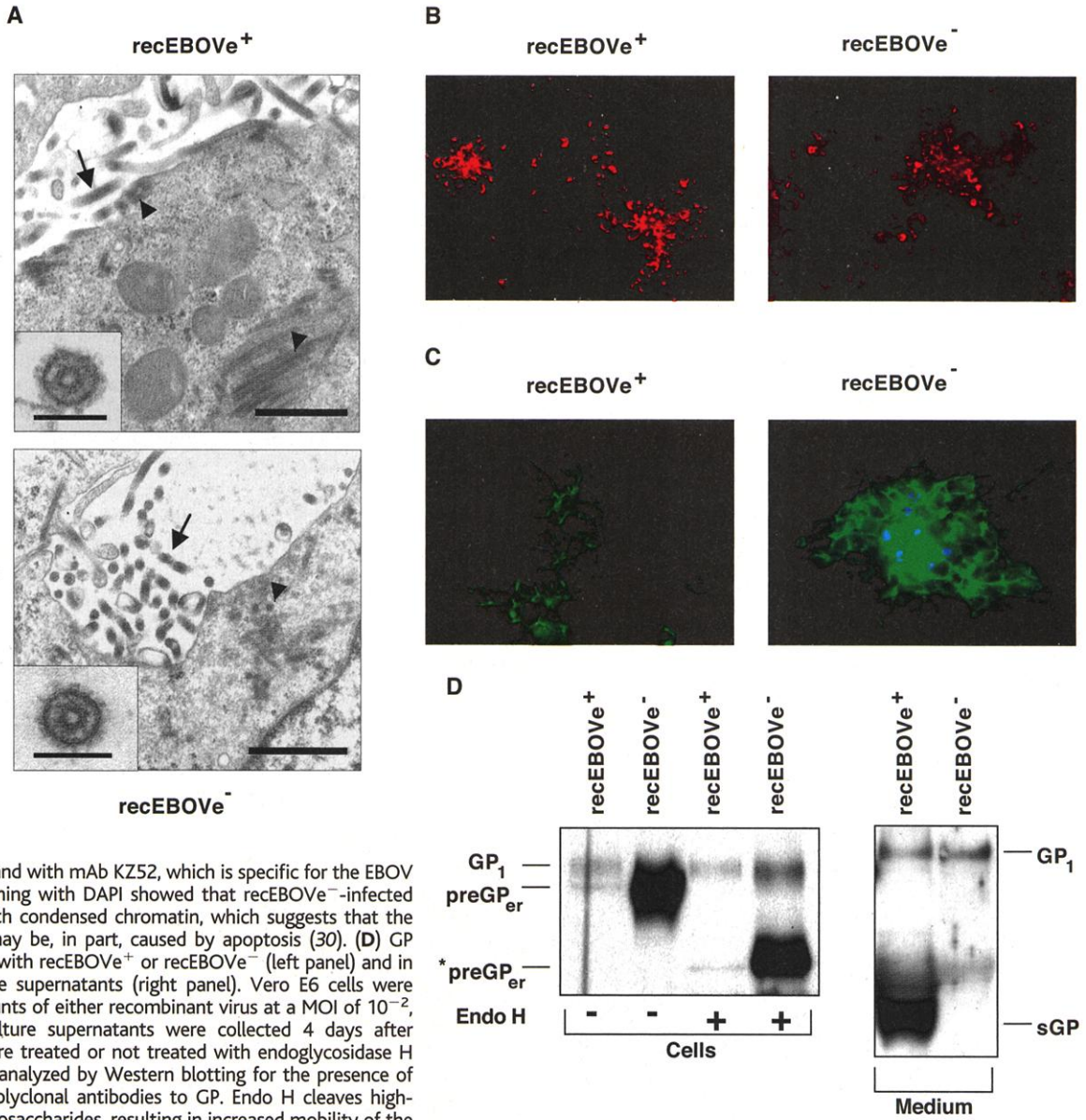

Fig. 3. Cells infected with recEBOVe$^-$ express more GP than cells infected with recEBOVe$^+$. (**A**) Electron microscopy of Vero cells infected with recombinant EBOVs. Ultrathin sections of recEBOVe$^+$- (top) or recEBOVe$^-$- (bottom) infected cells (*27*, *28*). EBOV nucleocapsids appear as thin strands or as circles in a regular arrangement (arrowheads); virus particles bud intensively from plasma membranes and are also seen extracellularly (arrows) (scale bar = 1000 nm). The insets show cross sections of virions (scale bar = 100 nm). Spikes formed by GP are seen on the surface of the virions. (**B** and **C**) Indirect immunofluorescence of Vero E6 cells infected with recEBOVe$^+$ (left panels) and recEBOVe$^-$ (right panels). The panels illustrate cells that were treated with mAb B6C5, which is specific to EBOV NP protein (B), and with mAb KZ52, which is specific for the EBOV GP protein (C) (*29*). Staining with DAPI showed that recEBOVe$^-$-infected cells contained nuclei with condensed chromatin, which suggests that the death of infected cells may be, in part, caused by apoptosis (*30*). (**D**) GP patterns in cells infected with recEBOVe$^+$ or recEBOVe$^-$ (left panel) and in the corresponding culture supernatants (right panel). Vero E6 cells were infected with equal amounts of either recombinant virus at a MOI of 10^{-2}, and cell lysates and culture supernatants were collected 4 days after infection. Cell lysates were treated or not treated with endoglycosidase H (Endo H) and were then analyzed by Western blotting for the presence of EBOV GP using rabbit polyclonal antibodies to GP. Endo H cleaves high-mannose (immature) oligosaccharides, resulting in increased mobility of the endoplasmic GP precursor (preGP$_{er}$) band. Mature GP$_1$ contains complex oligosaccharides and therefore showed resistance to the Endo H treatment. Culture supernatants were analyzed by Western blotting for the presence of EBOV GPs using antibodies to GP. Similar amounts of GP were released into the culture medium by each recombinant EBOV.

mic reticulum or in an early Golgi compartment. These observations support the interpretation that infected cells have a limited capacity to process the highly glycosylated transmembrane GP of EBOV. Overexpression of GP, which occurs with recEBOVe$^-$, might therefore lead to cell death by exhausting the processing machinery of the cells. Transcriptional editing of the GP gene may therefore be an important factor in the pathogenicity of EBOV infection, because by restricting cytotoxicity, it is likely to enhance virus loads and to promote the spread of infection in the organism. In addition, evidence has recently been presented for a cytotoxic function of recombinant GP that has been allocated either to the GP$_2$ subunit (*8*) or to the so-called mucinlike region in the ectodomain of GP$_1$ (*9*). Neither model—intracellular accumulation or a specific cytotoxicity domain—excludes the other. It is clear from our data that cytotoxicity depended on the level of GP expression, and it appears that editing of the EBOV GP gene, although not being required for virus replication, is evolutionarily linked with the need to control cytotoxicity. In addition, our data showed that sGP was unnecessary for replication of EBOV in cell culture. However, this does not exclude sGP from playing a role as a biologically active protein in infection in humans or in the as-yet-unknown natural host.

With the help of this system for recovering EBOV, we will be able to gain new insight onto the role of each viral gene in the replication process and to open new avenues for prevention and treatment of the infection.

References and Notes

1. C. J. Peters, A. Sanchez, P. E. Rollin, T. G. Ksiazek, F. A. Murphy, in *Fields Virology*, B. N. Fields *et al.*, Eds. (Raven, Philadelphia, ed. 3, 1996), pp. 1161–1176.
2. H. Feldmann, M. P. Kiley, in *Marburg and Ebola Viruses*, H.-D. Klenk, Ed. (Springer-Verlag, Berlin, 1999), pp. 1–21.
3. V. E. Volchkov *et al.*, *Virology* **214**, 421 (1995).
4. A. Sanchez, S. G. Trappier, B. W. Mahy, C. J. Peters, S. T. Nichol, *Proc. Natl. Acad. Sci. U.S.A.* **93**, 3602 (1996).
5. A. Takada *et al.*, *Proc. Natl. Acad. Sci. U.S.A.* **94**, 14764 (1997).
6. H. Ito, S. Watanabe, A. Sanchez, M. A. Whitt, Y. Kawaoka, *J. Virol.* **73**, 8907 (1999).
7. V. E. Volchkov, H. Feldmann, V. A. Volchkova, H.-D. Klenk, *Proc. Natl. Acad. Sci. U.S.A.* **95**, 5762 (1998).
8. S. Y. Chan, M. C. Ma, M. A. Goldsmith, *J. Gen. Virol.* **81**, 2155 (2000).
9. Z. Y. Yang *et al.*, *Nature Med.* **6**, 886 (2000).
10. A. Sanchez *et al.*, *J. Infect. Dis.* **179** (suppl. 1), 164 (1999).

11. A. Bukreyev, V. E. Volchkov, V. M. Blinov, S. V. Netesov, *FEBS Lett.* **323**, 183 (1993).
12. C. Will *et al.*, *J. Virol.* **67**, 1203 (1993).
13. See Web Fig. 1 on Science Online at www.sciencemag.org/cgi/content/full/1057269/DC1.
14. V. E. Volchkov *et al.*, *J. Gen. Virol.* **80**, 355 (1999).
15. V. E. Volchkov, V. M. Blinov, S. V. Netesov, *FEBS Lett.* **305**, 181 (1992).
16. The plasmid pFL-EBOVe$^+$ was designed to place the T7 promoter adjacent to the viral leader region, and the viral trailer region was constructed to be adjacent to a ribozyme sequence followed by tandem terminators of T7 transcription. In this case, the correct 3′ end of the transcribed EBOV antigenome, free of additional nucleotides, was generated by self-cleavage of the ribozyme (*24*). To increase the transcriptional activity of the T7 RNA polymerase, an additional guanosine residue was introduced between the promoter of the T7 polymerase and the first residue of the EBOV genome (*25*). The length of the encoded antigenome (FL-EBOVe$^+$) is therefore increased by 1 nt compared to that of the wild-type virus (GenBank accession number, AF086833). The size of the full-length antigenome encoded by the plasmid pFL-EBOVe$^-$ was 1 nt longer than that encoded by pFL-EBOVe$^+$ and 2 nt longer than the size of the genome of the wild-type virus because of the insertion of additional adenosine residues at the editing site. Mutations at the GP gene editing site were introduced into the plasmid pKSS25 by site-directed mutagenesis using the primers 5′-GG GAAACTAAGAAGAAACCTCACTAG and 5′-CTAGTGAGGTTTCTTCTTAGTTTCCC.
17. The Sal I restriction site (GTCGAC) located in the GP gene at position 6180 was mutated by site-directed mutagenesis using the pair primers 5′-GGTTAGTGATGTAGATAA ACTAGTTTG and 5′-CAAACTAGTTTATC TACATCACTAACC. This mutation is silent. In addition, an accidental mutation in a nontranslated region of the L gene (A → U at position 18227) was found after complete sequence analysis of the final plasmid clones.
18. U. J. Buchholz, S. Finke, K.-K. Conzelmann, *J. Virol.* **73**, 251 (1999).
19. E. Mühlberger, M. Weik, V. E. Volchkov, H.-D. Klenk, S. Becker, *J. Virol.* **73**, 2333 (1999).
20. BSR T7/5 cells were grown overnight to about 60 to 80% confluency in 25-cm^2 flasks in 1× Glasgow medium supplemented with 10% NCS (newborn calf serum). One hour before transfection, cells were washed twice with medium without NCS. Cells were transfected with a plasmid mixture containing 2 μg of full-length plasmid (pFL-EBOVe+), 0.2 μg of pT/VP30EBOV, 0.5 μg of pT/VP35EBOV, 0.5 μg of pT/NPEBOV, and 1 μg of pGEM-LEBOV (*14*, *19*). Transfection experiments were carried out with a Fusion 6 reagent (transfection protocol supplied by Roche). The transfection medium was removed at 8 hours after transfection; cells were washed and maintained in Glasgow medium containing 2.5% NCS for 6 to 9 days after transfection. On average, in each rescue experiment, approximately 100 foci of rounded cells were observed in the cell culture flask (about 1×10^5 to 2×10^5 cells). That means that one in approximately 10^3 cells allowed the formation of viral particles. However, virus release from BHK cells was extremely low, and amplification of recombinant EBOV on Vero cells was necessary before further analysis. Determination of the virus titers by plaque formation showed that about 200 infectious particles were recovered from the average rescue experiment.
21. E. Mühlberger, B. Lötfering, H.-D. Klenk, S. Becker. *J. Virol.* **72**, 8756 (1998).
22. For RT-PCR, RNA from culture supernatants of Vero E6 cells infected with individual plaques of recEBOV-e$^+$, recEBOV-e$^-$, or wild-type EBOV was purified (with the Rneasy Kit, Qiagen) when an extensive CPE was observed. To verify the identity of the recombinant viruses, the region containing the marker restriction site Sal I shown in Fig. 1 was amplified by RT-PCR using primers 5′-AGTCATCCACAATAGCACAT and 5′-TCGTGGCAGAGGGAGTGT. The PCR products were only seen when the RT step was performed, which confirms that they were derived solely from viral RNA and not from contaminating cDNA. PCR products were consistent with the predicted size of 1298 bp. Demonstration of the presence or absence of a Sal I site in authentic EBOV and recEBOV was performed on 1% agarose gel. Sal I digestion products were consistent with the predicted sizes of 1130 and 168 bp. In addition, the sequences at the restriction site marker and at the GP gene editing site were confirmed by partial nucleotide sequencing of RT-PCR products.
23. S. Vidal, J. Curran, D. Kolakofsky, *EMBO J.* **9**, 2017 (1990).
24. A. T. Perrotta, M. D. Been, *Nature* **350**, 434 (1991).
25. A. K. Pattnaik, L. A. Ball, A. W. LeGrone, G. W. Wertz, *Cell* **69**, 1011 (1992).
26. V. E. Volchkov *et al.*, *Virology* **277**, 147 (2000).
27. For electron microscopy, 72 hours after infection, control and virus-infected cells were fixed with Hanks' balanced salt solution (HBSS) containing 2.5% glutaraldehyde, postfixed with HBSS containing 1% osmium tetraoxide, dehydrated, and embedded in Epon. Ultrathin sections were cut, placed on 200-mesh copper electron microscopy grids, stained with uranyl acetate and lead citrate, and examined with a Zeiss 109 transmission electron microscope at 80 kV.
28. See Web Fig. 2 on Science Online at www.sciencemag.org/cgi/content/full/1057269/DC1.
29. For immunofluorescent staining, Vero E6 cells were infected at a multiplicity of infection (MOI) of 10^{-2} and were processed 3 days later for indirect immunofluorescence analysis. Cells grown on coverslips were washed with phosphate-buffered saline (PBS) solution, fixed with 4% paraformaldehyde at 4°C for 24 hours, and permeabilized with 0.1% Triton X-100 in PBS for 5 min. The nonspecific binding was blocked by blocking buffer (2% bovine serum albumin, 5% glycerol, and 0.2% Tween-20 in PBS), and cells were then incubated with 100 mM glycine for 10 min, washed with PBS, and incubated at 4°C for 18 hours with the respective antibodies [human monoclonal antibody (mAb) KZ52, which is specific for the EBOV GP (dilution 1:100 in blocking buffer); and mouse mAb B6C5, which is specific to EBOV NP (dilution 1:10 in blocking buffer)]. Subsequently, cells were washed three times with PBS and stained with fluorescein isothiocyanate–conjugated goat anti-human immunoglobulin G (IgG) (diluted 1:50 in blocking buffer) or with rhodamine-conjugated goat anti-mouse IgG (1:100 in blocking buffer) for 1 hour at room temperature. Nuclear counterstaining was performed with 4′,6′-diamidino-2-phenylindole (DAPI) (0.1 μg/ml). Finally, cells were washed three times with PBS, dipped into dH2O, covered with mounting medium, coverslipped, and examined with a fluorescence microscope (Axiomat, Zeiss) with digital photographic equipment for taking images (Spot camera system, version 2.1.2, Diagnostic Instruments).
30. See Web Fig. 3 on Science Online at www.sciencemag.org/cgi/content/full/1057269/DC1.
31. All experiments involving infectious EBOV were carried out in biosafety level 4 (BSL4) laboratories at the Institute of Virology in Marburg, Germany, and at the Jean Merieux P4 Research Center in Lyon, France. We thank D. Burton and P. Parren for providing mAb KZ52A; S. Becker for mAb B6C5; K.-K. Conzelmann for the BSR T7/5 cell line; A. Sergeant and E. Derrington for critical reading of the manuscript; and C. Laukel and M. Rossi for expert technical help. M.W. was supported as a recipient of a fellowship from the Boehringer Ingelheim Fonds. This work was supported in part by the Deutsche Forschungsgemeinschaft (SFB 286), the Fonds der Chemischen Industrie, and INSERM; and by a grant from the Fondation pour la Recherche Medicale to V.E.V.

8 November 2000; accepted 22 January 2001
Published online 1 February 2001;
10.1126/science.1057269
Include this information when citing this paper.

Genetic Correlates of Musical Pitch Recognition in Humans

Dennis Drayna,[1]* Ani Manichaikul,[1] Marlies de Lange,[2] Harold Snieder,[2]† Tim Spector[2]

We used a twin study to investigate the genetic and environmental contributions to differences in musical pitch perception abilities in humans. We administered a Distorted Tunes Test (DTT), which requires subjects to judge whether simple popular melodies contain notes with incorrect pitch, to 136 monozygotic twin pairs and 148 dizygotic twin pairs. The correlation of DTT scores between twins was estimated at 0.67 for monozygotic pairs and 0.44 for dizygotic pairs. Genetic model-fitting techniques supported an additive genetic model, with heritability estimated at 0.71 to 0.80, depending on how subjects were categorized, and with no effect of shared environment. DTT scores were only weakly correlated with measures of peripheral hearing. This suggests that variation in musical pitch recognition is primarily due to highly heritable differences in auditory functions not tested by conventional audiologic methods.

The perception of pitch requires both the ear, which receives auditory signals, and the brain, which performs substantial processing of auditory signals to produce a perceived pitch (*1*–*3*). Although the general features of human pitch processing have been well described, the precise cellular and molecular mechanisms involved remain largely obscure. One approach to understanding the mechanisms of pitch perception is to use genetic methods that exploit naturally occurring variation in pitch perception ability (*4*). If such variability is due to genetic factors, linkage and positional cloning studies could identify genes that encode the components of the pitch perception apparatus (*5*). To examine the genetic contributions to musical pitch

[1]National Institute on Deafness and Other Communication Disorders, National Institutes of Health, 5 Research Court, Rockville, MD 20850, USA. [2]Twin Research and Genetic Epidemiology Unit, St. Thomas' Hospital, London, SE1 7EH, UK.

*To whom correspondence should be addressed.
†Present address: Georgia Prevention Institute, Medical College of Georgia, Building HS-1640, Augusta, GA 30912, USA.